OPEN

Correspondence and
requests for materials
should be addressed to
W.-X.Z. (wxzhou@
ecust.edu.cn) or H.E.S.
(hes@bu.edu)

Systemic risk and spatiotemporal dynamics of the US housing market

Hao Meng[1,2], Wen-Jie Xie[1,2], Zhi-Qiang Jiang[1,3], Boris Podobnik[4,5,6,7], Wei-Xing Zhou[1,2,3] & H. Eugene Stanley[4]

[1]School of Business, East China University of Science and Technology, Shanghai 200237, China, [2]School of Science, East China University of Science and Technology, Shanghai 200237, China, [3]Research Center for Econophysics, East China University of Science and Technology, Shanghai 200237, China, [4]Center for Polymer Studies and Department of Physics, Boston University, Boston, MA 02215, USA, [5]Zagreb School of Economics and Management, 10000 Zagreb, Croatia, [6]Faculty of Civil Engineering, University of Rijeka, 51000 Rijeka, Croatia, [7]Faculty of Economics, University of Ljubljana, 1000 Ljubljana, Slovenia.

Housing markets play a crucial role in economies and the collapse of a real-estate bubble usually destabilizes the financial system and causes economic recessions. We investigate the systemic risk and spatiotemporal dynamics of the US housing market (1975–2011) at the state level based on the Random Matrix Theory (RMT). We identify richer economic information in the largest eigenvalues deviating from RMT predictions for the housing market than for stock markets and find that the component signs of the eigenvectors contain either geographical information or the extent of differences in house price growth rates or both. By looking at the evolution of different quantities such as eigenvalues and eigenvectors, we find that the US housing market experienced six different regimes, which is consistent with the evolution of state clusters identified by the box clustering algorithm and the consensus clustering algorithm on the partial correlation matrices. We find that dramatic increases in the systemic risk are usually accompanied by regime shifts, which provide a means of early detection of housing bubbles.

B ecause houses and apartments are tradeable and are commonly used in speculations, they are considered as a special kind of commodity. As time passes the house prices boom and bust. Because the housing market is closely related to the financial system and plays a crucial role in economies, a crash of the housing market usually has disastrous consequences, causing financial crisis and economic recession. Recent examples include the 1997–1998 Asian crisis[1–3] and the 2007–2012 global financial tsunami followed by the 2008–2012 global recession and the European sovereign-debt crisis, none of which has ended[4]. When the correlations among the constituents of a market become stronger and the ripple effect increases[5], prices tend to converge[6] and the systemic risk increases. However, there is evidence showing that alternative measures based on eigenvalues and eigenvectors of the correlation matrix outperform the average correlation in characterizing market integration[7], quantifying systemic risks measured by means of the absorption ratio[8], and constructing profitable investment portfolios[8,9]. Hence, it is extremely important to understand the spatiotemporal dynamics of housing markets through an investigation of the correlation matrix of price growth rates.

The correlation matrices of stock returns and indices have been widely studied in different markets[10]. The studies have employed variety of methods ranging from the minimal spanning trees[11], the planar maximally filtered graph[12] based on distance matrices, to RMT[13,14]. All methods can be used to identify constituent clusters in financial systems[10]. When RMT is used to investigate the correlation structure of financial markets, the largest eigenvalue serves to explain the collective behavior of the market, and other eigenvalues are commonly used to explain clustering of stocks or indices into groups with specific traits.

The correlation matrices of housing markets are rarely studied, mainly due to the short length of house price indices, where the sampling frequency is usually either monthly or quarterly. Using the RMT framework at the state level, we investigate the spatiotemporal dynamics of the US housing market. We analyze the All-Transactions Indices of the 50 states and the District of Columbia published by the Federal Housing Finance Agency, which estimate sales prices and appraisal data. The data are recorded quarterly from 1975/Q1 to 2011/Q4, giving a total of 148 values.

We denote $S_i(t)$ the quarterly housing price index (HPI) of US state i at time t. The logarithmic return at time t is defined as

$$r_i(t) = \ln S_i(t) - \ln S_i(t-1). \tag{1}$$

For each moving window $[t-s+1, t]$ at time t of size s, we compute the correlation matrix $\mathbf{C}(t)$, whose element C_{ij} is the Pearson correlation coefficient between the return time series of US states i and j,

$$C_{ij}(t) = \frac{1}{\sigma_i \sigma_j} \sum_{k=t-s+1}^{t} \left[r_i(k) - \mu_i\right]\left[r_j(k) - \mu_j\right], \quad (2)$$

where μ_i and μ_j are the sample means and σ_i and σ_j are the standard deviations of the two states i and j respectively.

Stock markets are characterized by both fast and slow dynamics[15,16]. To estimate the empirical correlation matrix and minimize the unavoidable statistical uncertainty, we use a large window containing a large number of data points. Although large windows reduce our ability to investigate the fast dynamics in correlation studies, the correlation matrix is no longer invertible[8,16] when the window size is smaller than the 51 time series in our study (50 states + DC), implying $s_{min} = 51$. We set the value at $s = 60$ quarters, giving us 89 moving windows for investigation.

Results

Correlation coefficient. Figure 1A shows the average correlation coefficient of Eq. 2 calculated for each year during the last two decades. In recent years the average correlation coefficient has sharply increased indicating that the US housing market has become strongly correlated. In the early years of the period studied, we find that only a small number of states exhibit correlated housing indices. In contrast, we find a sharp increase in housing market correlations over the past decade, indicating that systemic market risk has also greatly increased.

Eigenvalues. An important topic in economic theory is whether housing market bubbles and financial bubbles in general are predictable. Figure 1B shows that the largest eigenvalue λ_1 of $\mathbf{C}(t)$ has trended upward since 1993. Note also that λ_1 sharply increased in 2008, coinciding with the bursting of the real estate bubble and the world-wide financial crisis of 2007–2010. Figure 1B shows that the largest eigenvalue λ_1 of $\mathbf{C}(t)$ is larger than the maximum eigenvalue

λ_{max} predicted by the RMT and is also larger than the critical value $\lambda_{5\%}$ of $f_{Rnd}(\lambda)$ (see *Methods*). For the second largest eigenvalue, we find $\lambda_2 > \lambda_{max}$ for all $\mathbf{C}(t)$ matrices and $\lambda_2 > \lambda_{5\%}$ for most $\mathbf{C}(t)$ matrices. We also find that the third largest eigenvalue λ_3 is larger than λ_{max} and $\lambda_{5\%}$ for most $\mathbf{C}(t)$ matrices, and the fourth largest eigenvalue λ_4 is larger than λ_{max} and $\lambda_{5\%}$ for part of the $\mathbf{C}(t)$ matrices. In contrast, the fifth largest eigenvalue λ_5 falls well within the range of $f_{RMT}(\lambda)$ and $f_{Rnd}(\lambda)$ (Fig. S2). The eigenvalues λ_1, λ_2 and λ_3 should thus contain information about nontrivial spatiotemporal properties of the US housing market dynamics. We also include λ_4 in our investigation.

In addition to using the average correlation coefficient we can also measure systemic risk using the absorption ratio $E_n = \sum_{i=1}^{n} \lambda_i / N$, which is a better approach because perfectly integrated markets can exhibit weak correlation[7–9]. Figure 1C shows the absorption ratio. Note that the increase in systemic risk is approximately linear, even during the burst of the housing bubble in 2007, indicating that the US housing market continues to be fragile and unstable.

Collective market effect and regime shifts. To investigate the possible collective market effect embedded in the deviating eigenvalues, we compare the returns of the eigenportfolio with the US HPI returns (see *Methods*). Before we proceed with the results for the housing market, we note that for stock markets $k_1 \neq 0$ and usually $k_1 \rightarrow 1$, and that $k_n \approx 0$ for $n > 1$[18]. Thus although the largest eigenvalue reflects the behavior of the stock market, the other eigenvalues do not.

In the following, we report that the RMT results obtained for the US housing market (Fig. 2 and Fig. S3), which differ substantially from the results obtained for stock markets. For the housing market, we observe that the correlation coefficient k_1 between $R(t')$ and $R_1(t')$ is large for the first four years, and then drops from 0.8354 (1993Q3) to 0.0655 (1993Q4). Then λ_1 gradually increases to 0.8826 (2002Q2) and 0.9593 (2002Q3) and remains close to 1. This behavior for λ_1 over time indicates that we can approximately identify three regimes for three time periods: [1989Q4, 1993Q3], [1993Q4, 2002Q2] and [2002Q3, 2011Q4] (see *Methods*). We find that the two regime-shift points in Fig. 2(a) virtually overlap with the first two local minima in the time dependence of λ_1 in Fig. 1. Therefore, in the regimes corresponding to the first and last time periods, the market effect quantified by the correlation coefficient k_1 is remarkable. In contrast, the market effect is much weaker in the second time period (Fig. S3). Within the second time period, we further identify a regime-shift point between 1997Q1 and 1997Q2, where k_1 drops from 0.6955 to 0.5879.

Figure 2(b) shows three regime shifts: 1993Q3–1993Q4, 1997Q1–1997Q2, and 2002Q2–2002Q3, which, surprisingly, are identical to those we found for λ_1. Figure 2(c) shows two regime shifts for the third largest eigenvalue λ_3: 1993Q3–1993Q4 and 1997Q1–1997Q2, which correspond to the first and second regime shifts found in eigenvalues λ_1 and λ_2. Figure 2(d) shows three regime shifts for the fourth largest eigenvalue λ_4: 1993Q3–1993Q4, 1999Q2–1999Q3, and 2002Q2–2002Q3, the first and third of which correspond to those found for eigenvalues λ_1 and λ_2.

Using the four regime shifts in Figs. 2(a)–2(d), we identify five eigenvalue regimes: $\mathcal{R}_1 = [1989Q4, 1993Q3]$, $\mathcal{R}_2 = [1993Q4, 1997Q1]$, $\mathcal{R}_3 = [1997Q2, 1999Q2]$, $\mathcal{R}_4 = [1999Q3, 2002Q2]$, and $\mathcal{R}_5 = [2002Q3, 2011Q4]$, which reveal an interesting US housing market dynamic. The five regimes are separated by four regime shift points: $\mathcal{T}_1$ between 1993Q3 and 1993Q4, $\mathcal{T}_2$ between 1997Q1 and 1997Q2, $\mathcal{T}_3$ between 1999Q2 and 1999Q3, and $\mathcal{T}_4$ between 2002Q2 and 2002Q3, where $\mathcal{T}_1$ is visible in the evolution of k_1, k_2, k_3 and k_4, $\mathcal{T}_2$ is visible in the evolution of k_1, k_2 and k_3, $\mathcal{T}_3$ is visible only in the evolution of k_4, and $\mathcal{T}_4$ is visible in the evolution of k_1, k_2 and k_4. The cross-validation of the four regime shift points in the four plots of Fig. 2 indicates that our identification of the different regimes is valid.
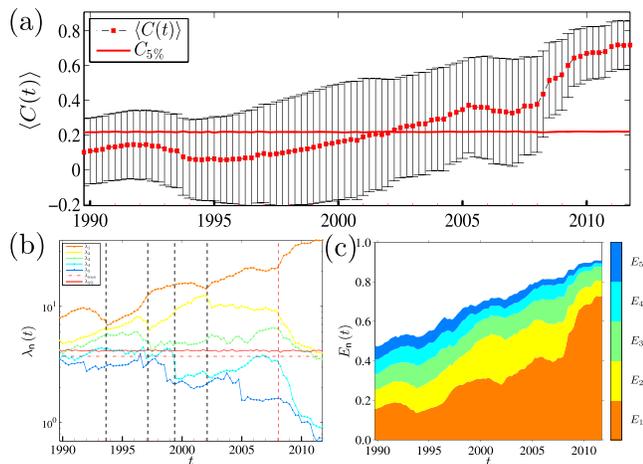

Figure 1 | Evolution of correlation coefficient, deviating eigenvalues and absorption ratio. (a) Evolution of the average correlation coefficient. The horizontal red line shows the critical value at significance level 5% of the correlation coefficient at each time t. The error bar is the standard deviation of the PDF at each time t. For the evolution of the PDF, see Fig. S1. (b) Evolution of the five largest eigenvalues λ_n of $\mathbf{C}(t)$ with $n = 1, 2, 3, 4$, and 5. The horizontal dot-dashed red line is the maximum eigenvalue λ_{max} predicted by the RMT and the horizontal red line represents the critical values $\lambda_{5\%}$ at the significance level of 5%. The five vertical dashed lines corresponding to the five regime-shift points. (c) Evolution of absorption ratio $E_n(t)$ for $n = 1, 2, 3, 4$, and 5.
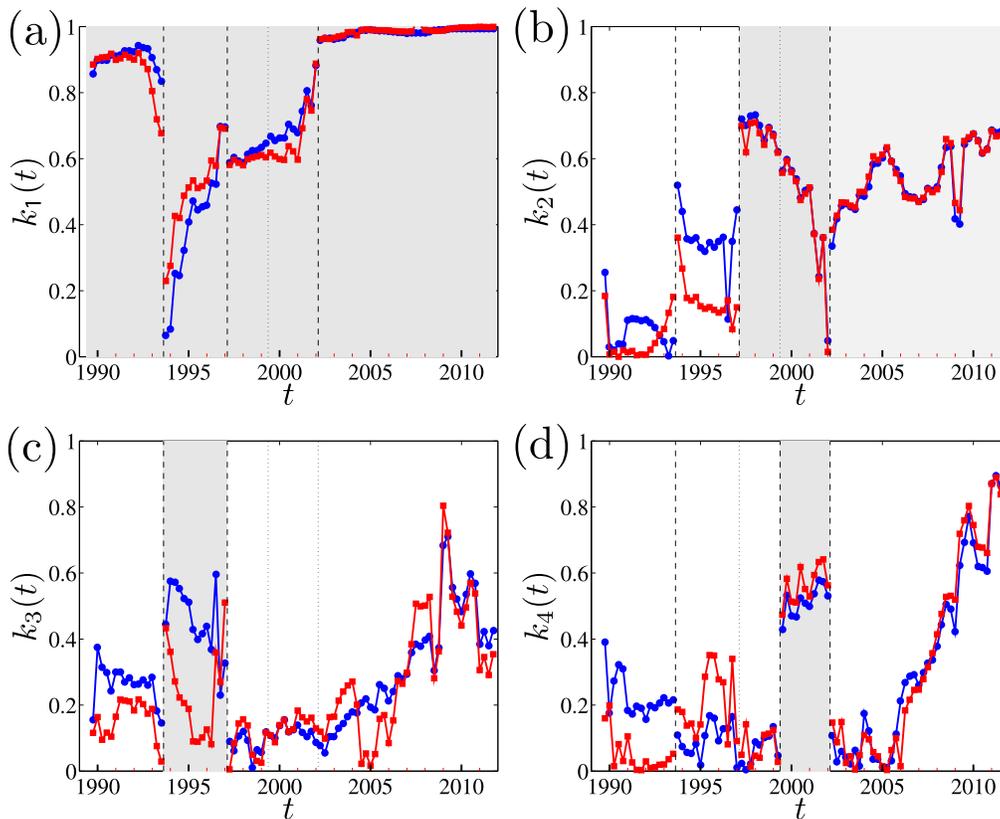
Figure 2 | Market effect hidden in the largest eigenvalues. Each plot shows the evolution of the correlation coefficient $k_n(t)$ between R_n and R in each moving window. The blue symbols are estimated using ordinary least-squares linear regression, while the red ones are estimated using robust fitting. The four vertical lines indicate four regime-shift points $\mathcal{T}_1$ between 1993Q3 and 1993Q4, $\mathcal{T}_2$ between 1997Q1 and 1997Q2, $\mathcal{T}_3$ between 1999Q2 and 1999Q3, and $\mathcal{T}_4$ between 2002Q2 and 2002Q3, separating five different regimes. The shading area in each plot means that the associated eigenvalue contains a market effect in the corresponding time period. See Fig. S3 for the scatter plots of R_n against R.

We find that in regime $\mathcal{R}_1$, only for the largest eigenvalue λ_1 is the market effect–quantified by the correlation coefficient k_1 between $R(t')$ and $R_1(t')$–substantially large (Fig. S3). In regime $\mathcal{R}_2$, the market effect for λ_1 becomes substantially weaker than in regime $\mathcal{R}_1$, and λ_3 exhibits a moderately stronger market effect only at some time t (Fig. S3). In regime $\mathcal{R}_3$, λ_1 and λ_2 exhibit a substantially stronger market effect than λ_3 and λ_4. In regime $\mathcal{R}_4$, λ_1, λ_2, and λ_4 exhibit a strong market effect. Finally, in regime $\mathcal{R}_5$, only λ_1 exhibits a strong market effect, while the rest of eigenvalues $\lambda_2 - \lambda_4$ do not. We thus find that the largest eigenvalue λ_1 almost always exhibits a market effect, whereas the other eigenvalues exhibit a market effect only infrequently, especially when the market effect becomes weak in λ_1.

Information contained in the eigenvectors associated with the largest eigenvalues. We find that the components of the eigenvector of the largest eigenvalue are positive in stock markets when the components exhibit small fluctuations over time, indicating a market effect. The rest of the eigenvectors of other largest eigenvalues describe different clusters of stocks or industrial sectors[18–20]. For the US housing market, we find that the eigenvectors of the largest eigenvalues contain much richer information (Fig. 3 and Fig. S4). The existence of five regimes $\mathcal{R}_1$ to $\mathcal{R}_5$ is clear and the eigenvector components persist in each regime (see *Methods*). Moreover, the graphical approach in Fig. 3 reveals that the regime $\mathcal{R}_5$ can be separated into two regimes at 2007Q1 to 2007Q2 according to the evolution of $\mathbf{u}_3$.

Starting with the first eigenvector $\mathbf{u}_1$, we study its components over time for different regimes. We find that in regime $\mathcal{R}_1$ almost all the components of $\mathbf{u}_1$ are positive. In contrast, Fig. 3 clearly shows

that after 1993Q4 and during the three regimes $\mathcal{R}_2$ to $\mathcal{R}_4$ many components of the first eigenvector $\mathbf{u}_1$ turn from positive to negative. During the period from 1993Q4 to 2002Q2, positive components of $\mathbf{u}_1$ approximately correspond to the states in the Eastern half of the US and with California and Arizona in the Western US. It means that the largest eigenvalue λ_1 partitions the states into two groups. Because the states with positive components are predominantly the states with high HPI values, λ_1 still exhibits a modest market effect. As time passes, transferring from regime $\mathcal{R}_4$ to regime $\mathcal{R}_5$, states with initially negative components turn from negative to positive components.

For the eigenvector $\mathbf{u}_2$ in the first two regimes $\mathcal{R}_1$ and $\mathcal{R}_2$ we find a comparable number of negligible positive and negative components, and it is not completely clear what information is contained in the US states with positive and negative components. At approximately 1997Q2 the number of states with negative $\mathbf{u}_2$ components drop significantly, leaving the majority of states with positive components that *reflect a market effect*. This predomination of positive components over negative components persists in $\mathcal{R}_3$ and $\mathcal{R}_4$. Beginning in late $\mathcal{R}_4$, the $\mathbf{u}_2$ components of Washington and California switch from positive to negative, and a few Northeastern states do the same. In regime $\mathcal{R}_5$, the two state clusters, one with positive and the other with negative $\mathbf{u}_2$ components, approximately correspond to states with low and high HPI growth rates, respectively, as identified by the super-exponential growth model[21].

In the evolution of the eigenvector $\mathbf{u}_3$, we find two interesting features. First, the majority of states in regime $\mathcal{R}_2$ have positive components, reflecting a modest market effect. Second, there is an evident subregime around 2007Q2, which surprisingly corresponds
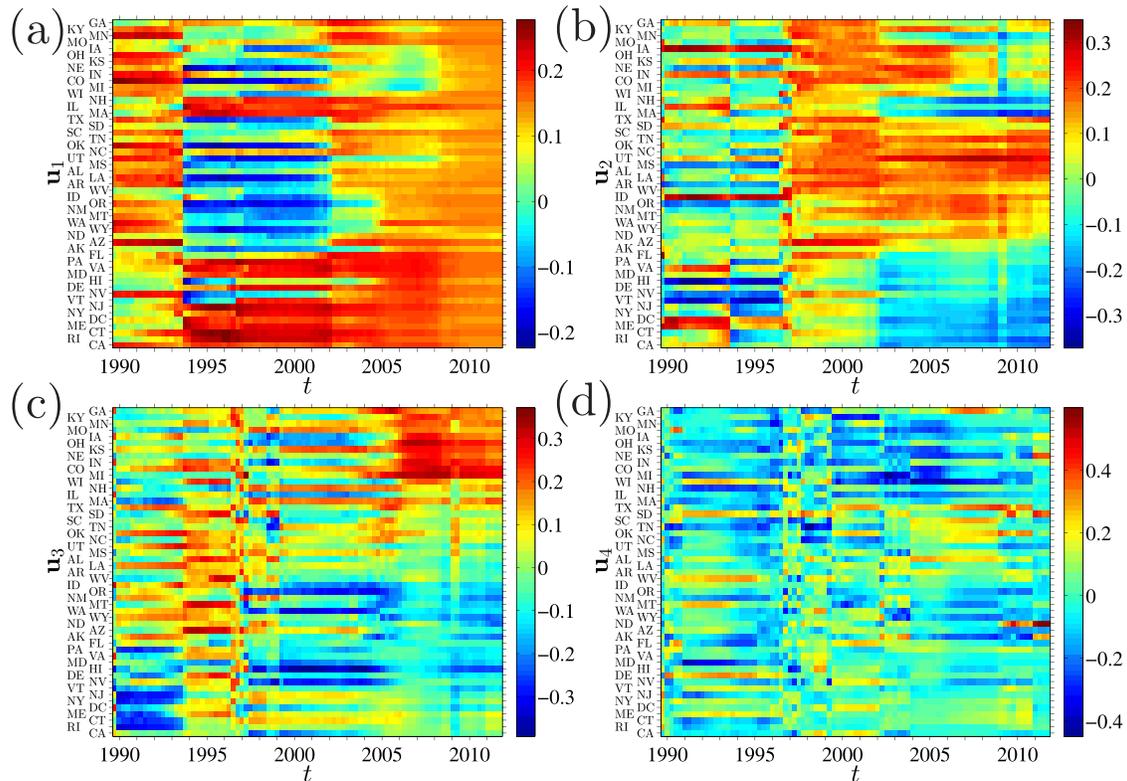
Figure 3 | Evolution of the eigenvectors of the largest eigenvalues. The five regimes $\mathcal{R}_1$ to $\mathcal{R}_5$ are visible. Moreover, we observe that the regime $\mathcal{R}_5$ can be separated into two regimes at 2007Q1 to 2007Q2 according to the evolution of $\mathbf{u}_3$.

to the onset of the primary US mortgage crisis. The information contained in other regimes is ambiguous, and it is difficult to extract clear information from the evolution of the fourth eigenvector $\mathbf{u}_4$.

Evolution of state clusters. To better understand the spatiotemporal dynamics of the US housing market at the state level, we partition the states into clusters for each time t. Because there is a strong market effect in the correlation matrices, the Pearson correlation coefficient between the return time series r_i and r_j of two US states i and j may not reflect their intrinsic relationship, but may reflect the influence of the overall US HPI return r_{us} on i and j[22,23]. We thus utilize a clustering algorithm that uses the corresponding partial correlation matrices $\mathbf{P}(t)$ by removing the market effect. In this way we obtain a partial correlation matrix $\mathbf{P}(t)$ and an affinity $\mathbf{A}(t)$ for each t (see *Methods*).

For each t, we rearrange the order of states in $\mathbf{P}(t)$ and $\mathbf{C}(t)$ to be the same as in $\mathbf{A}(t)$. The evolution of the three matrices is illustrated in Fig. S5. In the early years represented by regions $\mathcal{R}_1$ and $\mathcal{R}_2$, we identify the state clusters (Fig. 4(a)) in which the number of states forming each cluster is relatively small (Fig. 4(b)) and the constituent states of the clusters are unstable (Fig. S5). These properties are consistent with the fact that the average cross-correlation level among US states is very low, indicating that the housing markets of different US states are to some extent isolated. With the development of the US housing market during the period 1996Q4–2002Q1, more US states enter two different clusters of significantly different sizes (Fig. 4(b)). This period roughly corresponds to the two regimes $\mathcal{R}_3$ and $\mathcal{R}_4$. During this period both clusters are relatively stable (Fig. 4(b) and Fig. S5). In regime $\mathcal{R}_5$ the smaller cluster further splits into two even smaller clusters which remain relatively stable. At approximately 2007Q2 the larger cluster splits into two clusters of comparable size, but shortly after the two smaller clusters merge back into one (Fig. S5). Finally we find three stable clusters of similar size that form the sixth regime $\mathcal{R}_6$.

For each window t there are up to four clusters of states and the number of states in each cluster varies from one window to the next. For each cluster, one of the four deviating eigenvalues makes a dominant contribution (Fig. 4(d)). We find that in regimes $\mathcal{R}_2$ and $\mathcal{R}_3$ the largest eigenvalue λ_1 participates in the cluster partitioning.

Figure 4(e) shows the spatiotemporal dynamics of the state clusters. The states in the red cluster tend to have larger price fluctuations (and a higher price value), and the states in the green cluster exhibit smaller HPI growth rate fluctuations (Fig. S6). In the earlier years ($\mathcal{R}_1$ and $\mathcal{R}_2$) the clusters are unstable with a large number of states shifting between clusters. During this period, the primary contribution to the green cluster comes from the third largest eigenvalue λ_3. In contrast, there are more eigenvalues contributing to the red cluster. In 1997 we find that two rapidly-forming large stable green and red clusters are dominated by λ_2 and λ_1, respectively. This phase-transition-like phenomenon in 1997 may have been evidence of a fast ripple effect within the US housing market. After 2005Q2 the red cluster splits into two smaller clusters for approximately two years and almost all of the clusters are dominated by λ_2. Beginning in 2007Q2 the green cluster partitions into two smaller clusters: the red and green clusters are still dominated by λ_2 and the new yellow cluster is dominated by λ_3. The time period of these two transitions corresponds to the downturn in the US housing market. In short, Fig. 4(e) shows the extreme complexity of the spatiotemporal dynamics of the US housing market.

In order to achieve a finer resolution as we characterize systemic risk, we divide the 51 time series into six clusters according to the state clusters shown in Fig. 4(e). We form a sample with six return time series, each being randomly chosen from a cluster. We use a moving window of eight quarters (two years) size to determine the eigenvalues of the correlation matrices of the sample. We repeat this procedure 50 times and average the corresponding eigenvalues. We find that the systemic risk increases sharply in the early 1990s and drops to a relatively low level in late 1990s (Fig. S7). The absorption
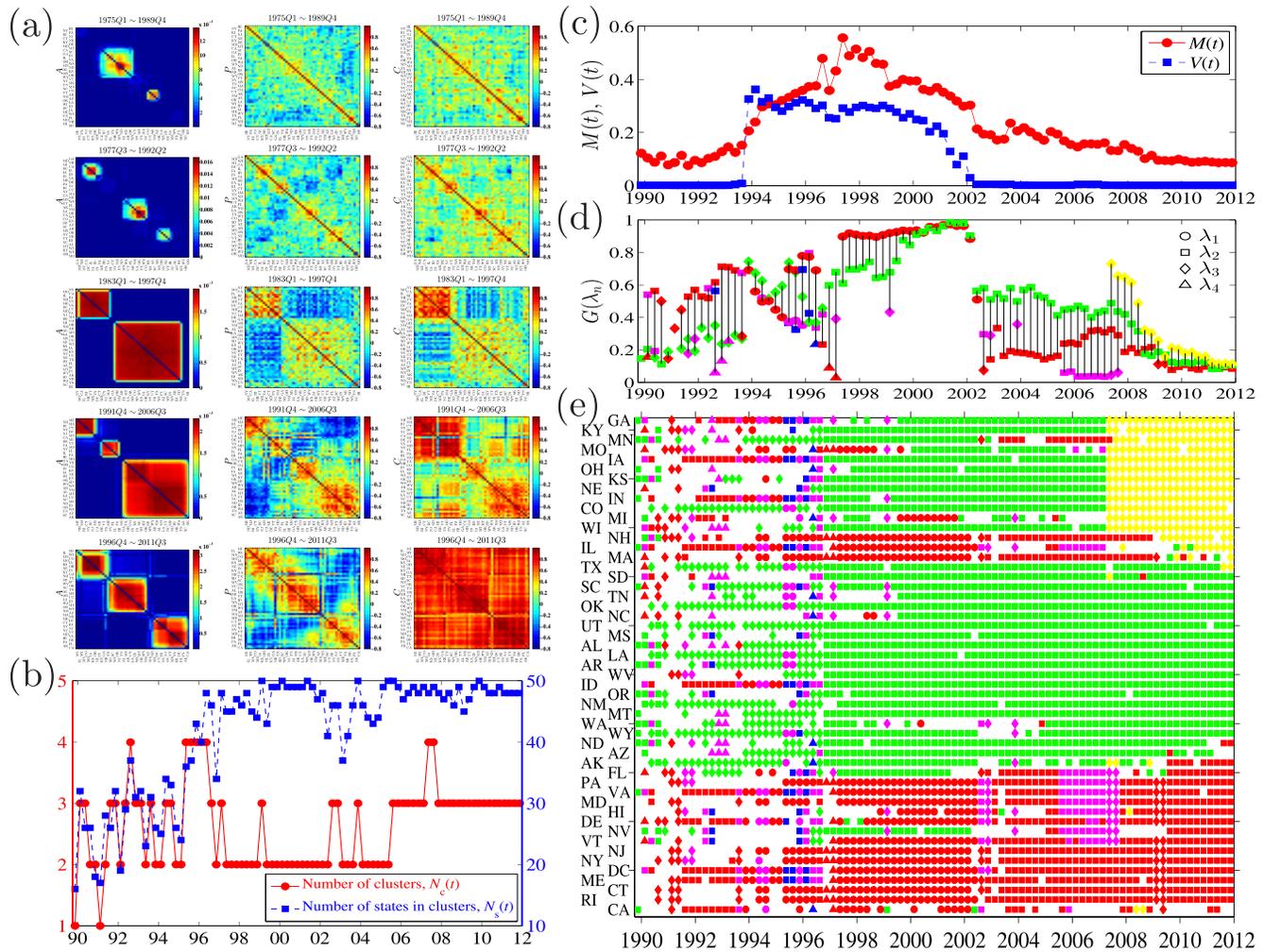
Figure 4 | Evolution of the states' clusters. (a) Typical affinity matrices $\mathbf{A}(t)$ (left column), partial correlation matrices $\mathbf{P}(t)$ (middle column), and correlation matrices $\mathbf{C}(t)$ (right column). The order of the states is the same for the three matrices in each row. The ending quarters t of the windows from top to bottom are 1989Q4, 1992Q2, 1997Q4, 2006Q3, and 2011Q3. (b) Number of clusters $N_c(t)$ and the corresponding number $N_s(t)$ of states included in the detected clusters for each window. (c) Evolution of modularity $M(t)$ and the squared sum $V(t)$ of negative components in $\lambda_1(t)$. (d) Maximal information ratio $G(\lambda_n)$ of certain eigenvalue λ_n contributed to a cluster. Each cluster is represented by a colorful symbol. The determination of symbols and their coloring is explained in *Methods*. (e) Evolution of states clusters, where the order of the states is the same as $\mathbf{A}(t)$ at $t = 2009Q3$. The states in a certain cluster are assigned with a cluster-specific colorful symbol and no symbol is assigned to those states not in any cluster. The colorful symbols have the same meaning as those in (d).

ratio increases dramatically in 2003 and remains historically high. Unlike the results of an analysis of 14 metropolitan housing markets in the United States[9], our analysis shows that the systemic risk is still at historically high levels after the housing bubble peaks.

Discussion

Using random matrix theory, we have investigated the complex spatiotemporal dynamics of the US housing market at the state level. Using long timescales, we divide the evolution of the market into three time periods. During the first time period (1989Q4 to 1997Q1) the market exhibits a low correlation, the largest eigenvalue reflects a market effect, and the next three largest eigenvalues contain partitioning information. During the second time period (1997Q2 to 2002Q2) the correlation among the states is still low and the market effect of the largest eigenvalue becomes weaker. We find that the largest eigenvalue contains partitioning information and that the deviating eigenvalues exhibit a weak market effect. During the last period, the largest eigenvalue exhibits a strong market effect and its partitioning function disappears, which corresponds to the fact that

market integration has become significantly stronger and exhibits sharply increasing average correlations. During this period, the partitioning of the states is primarily caused by the second largest eigenvalue. After the subprime crisis, the third largest eigenvalue exhibits a partitioning function.

These regime shifts reflect the abrupt increases in systemic risk that took place in the US housing market. Figures 4(b) and 4(d) show that in 1997 most states were gathered into two clusters. Thus we conjecture that the housing bubble that burst in 2007 had begun to inflate as early as 1997. This finding is consistent with and provides convincing evidence for our conclusion based on the evolution of the absorption ratio[9].

Note that there are both positive and negative components in the eigenvectors of the deviating eigenvalues for most time windows. When the components of an eigenvector have the same sign, it usually reflects a market effect. When an eigenvector has both positive and negative components, especially when their amounts are comparable, the eigenvector may reflect either geographical information or differences in house price growth rates or both. The information

contained in the signs of the eigenvector components has recently been reported for stock markets[27–29]. However, the US housing market appears more complex than stock markets.

During the evolution of the US housing market, we observe that prices diffuse in complex ways that do not require geographical clusters[30]. This differs from worldwide stock markets, which exhibits clear geographical clustering[16]. The splitting and merging of clusters indicate that there is no national convergence of house prices. Furthermore, the model in Ref. 6, in which there are several clusters within which the prices converge is too simple, so we have used a different approach for state clustering. We thus conjecture that there are different classifications for converging clusters in different time periods.

Methods

Determining deviating eigenvalues. For each t larger or equal to $t = 1990/Q1$, we calculate the correlation matrix $\mathbf{C}(t)$ and compute its 51 eigenvalues $\{\lambda_n : n = 1, \cdots, 51\}$. Then we sort the eigenvalues $\{\lambda_n\}$ in descending order and calculate the corresponding eigenvectors $\mathbf{u}_n(t) = [u_{n,1}(t), \cdots, u_{n,51}(t)]^{\mathrm{T}}$.

If M is a $T \times N$ matrix with mean 0 and variance $\sigma^2 = 1$, we define $\mathbf{C} = \frac{1}{T}\mathbf{M}^{\mathrm{T}}\mathbf{M}$. In the limit $N \rightarrow \infty$, $T \rightarrow \infty$ where $Q = T/N \geq 1$ is fixed, the probability density $f_{\mathrm{RMT}}(\lambda)$ of eigenvalues λ of matrix $\mathbf{C}$ is $f_{\mathrm{RMT}}(\lambda) = \frac{Q}{2\pi}\sqrt{(\lambda_{\max} - \lambda)(\lambda - \lambda_{\min})/\lambda}$, where $\lambda \in [\lambda_{\min}, \lambda_{\max}]$ and $\lambda_{\min,\max} = 1 + 1/Q \pm 2\sqrt{1/Q}$[17,13,18]. If an eigenvalue λ is greater than $\lambda_{\max}$– and thus deviates from the prediction of the RMT–its eigenvector frequently contains valuable information about market dynamics.

In real-world data, however, the limit conditions $N \rightarrow \infty$ and $T \rightarrow \infty$ are never fulfilled and some finite-size effect should be included in the RMT studies. In order to identify the deviating eigenvalues, we thus randomize the housing index time series to eliminate any temporal correlations. We then calculate a new correlation matrix $\mathbf{C}_{\mathrm{Rnd}}$ from the randomized return time series, and compute the corresponding 51 eigenvalues. Repeating this procedure 1000 times we obtain a total of 51,000 eigenvalues based on which we calculate the probability density of eigenvalues $f_{\mathrm{Rnd}}(\lambda)$. Although the density functions $f_{\mathrm{RMT}}(\lambda)$ and $f_{\mathrm{Rnd}}(\lambda)$ overlap to a great degree, they exhibit some differences in the right-hand tail. We find that $f_{\mathrm{Rnd}}(\lambda)$ is not bounded by the maximum eigenvalue $\lambda_{\max}$ predicted by the RMT (Fig. S2). This is the case because the HPI returns have fat tails. We retain only the eigenvalues that come from the distribution $f_{\mathrm{Rnd}}(\lambda)$ with a probability smaller than 5% and we denote the critical value to be $\lambda_{5\%}$.

Construction of eigenportfolio. For each eigenvalue λ_n we construct its eigenportfolio, the returns of which we calculate by

$$R_n(t') = \mathbf{u}_n^{\mathrm{T}}(t') \cdot \mathbf{r}(t') \qquad (3)$$

where $t' = t - s + 1, \cdots, t$, and $\mathbf{r}(t') = [r_1(t'), \cdots, r_{51}(t')]^{\mathrm{T}}$ is a vector whose components are state-level HPI returns defined in Eq. 1. To evaluate the collective market effect embedded in λ_n, we investigate the following linear regressive model between $R_n(t')$ and the return $R(t')$ of the US HPI

$$R_n(t') = k_n(t)R(t') + \epsilon(t') \qquad (4)$$

where R_n and R are normalized respectively to zero mean and unit variance[18], and $k_n(t)$ is the correlation coefficient between R_n and R in time t'. If k_n differs significantly from 0, we assume the eigenvalue λ_n contains a market effect because the corresponding eigenportfolio is correlated with the entire market[18]. The market effect is stronger if k_n is larger. To estimate the value of k_n, we perform an ordinary least-squares (OLS) linear regression together with a robust regression. Since the results and conclusions for both methods are qualitatively the same, we limit our discussion to the OLS results.

Partial correlations and state clustering. The partial correlation coefficient P_{ij} between r_i and r_j with respect to r_{us} can be calculated[24,23]

$$P_{ij} = \frac{C_{ij} - C_{i,\mathrm{us}}C_{j,\mathrm{us}}}{\sqrt{\left(1 - C_{i,\mathrm{us}}^2\right)\left(1 - C_{j,\mathrm{us}}^2\right)}}, \qquad (5)$$

where $C_{i,\mathrm{us}}$ ($C_{j,\mathrm{us}}$) is the Pearson correlation coefficient between r_i (r_j) and r_{us}. For each partial correlation matrix $\mathbf{P}(t)$, we combine the box clustering and consensus clustering methods to search for clusters of states[25,26]. We first determine the optimal ordering of $\mathbf{P}(t)$ by identifying the largest elements in $\mathbf{P}(t)$ close to the diagonal, where the simulated annealing approach is adopted to minimize the cost function

$$Q = \sum_{i,j=1}^{51} |i - j| P_{ij}(t). \qquad (6)$$

We then use a greedy algorithm to partition clusters of states and isolated states[25]. We repeat this procedure 200 times and obtain 200 partitions. We construct an affinity matrix $\mathbf{A}'$ whose element A'_{ij} is the number of partitions in which i and j are assigned to the same cluster, divided by the number of partitions 200. Finally we apply the clustering method to the affinity matrix $\mathbf{A}'$, resulting in a final partition $\mathbf{A}(t)$[26]. For each t, we rearrange the order of states in $\mathbf{P}(t)$ and $\mathbf{C}(t)$ to be the same as in $\mathbf{A}(t)$.

Identification of different regimes. To identify different regimes, we locate abrupt changes in the evolution of different variables. The first class of variables is the degree of market effect quantified by k_n for the deviating eigenvalues as shown in Fig. 2. If the absolute change $|k_n(t + 1) - k_n(t)|$ is significantly greater than the average of the absolute changes around t, t is identified as a possible regime-shifting point. For the evolution of eigenvectors in Fig. 3, if there appears to be significantly less similarity between two successive eigenvectors $\mathbf{u}_n(t)$ and $\mathbf{u}_n(t + 1)$, t is a possible regime-shifting point. This similarity criterion can also be applied to the evolution of state clusters as shown in Fig. 4(e). If the identified regime-shifting points overlap, their presence is more convincing. Comparing the results from different variables can thus serve as a method of cross-validation. Thus to design a reliable method of regime identification we clearly need to construct mathematical models that include the kind of regime-shifting seen in the US housing market.

Determination of symbols in Fig. 4(d). We assign the symbol for each cluster according to the contribution made by the eigenvalues. Note that the correlation matrix $\mathbf{C}(t)$ can be decomposed as[31,32]

$$\mathbf{C}(t) = \sum_{n=1}^{51} \mathbf{C}_{\lambda_n}(t) = \sum_{n=1}^{51} \lambda_n(t)\mathbf{u}_n(t)\mathbf{u}_n^{\mathrm{T}}(t), \qquad (7)$$

where $\mathbf{C}_{\lambda_n}(t) = \lambda_n(t)\mathbf{u}_n(t)\mathbf{u}_n^{\mathrm{T}}(t)$ is the matrix associated with λ_n, and its element is $C_{\lambda_n,ij}(t) = \lambda_n(t)u_{n,i}(t)u_{n,j}(t)$. We define the information ratio of λ_n in a certain cluster $\mathcal{C}(t)$ as

$$G(\lambda_n, \mathcal{C}(t)) = \frac{\sum_{i,j \in \mathcal{C}(t)} C_{\lambda_n,ij}(t)}{\sum_{i,j \in \mathcal{C}(t)} C_{ij}(t)}, \qquad (8)$$

which is the relative contribution of λ_n to $\mathcal{C}(t)$, and the maximum information ratio $G(\lambda_n)$ can be easily determined. Since almost all the components of u_1 are positive in regimes $\mathcal{R}_1$, $\mathcal{R}_5$, and $\mathcal{R}_6$ (Fig. 4(c)), the partitioning function of λ_1 is weak. In these time periods, the modularity defined in Ref. 33, 34 is also relatively small. We thus exclude λ_1 from the determination of $G(\lambda_n)$ in these three regimes. If $\lambda_n(t)$ makes the largest contribution to cluster $\mathcal{C}(t)$ (i.e., $G(\lambda_n, \mathcal{C}(t))$) is maximal), then an eigenvalue-specific symbol is assigned to $\mathcal{C}(t)$: circle (●) for λ_1, square (■) for λ_2, diamond (◆) for λ_3, and triangle (▲) for λ_4.

Coloring the states in Fig. 4(e). For a given time t, states belonging to the same cluster are marked with the same color and states belonging to different clusters are marked with different colors. For the sake of simplicity, we define for each t a color configuration vector Φ_t, the elements of which correspond to the 51 states in a predetermined order. The elements of Φ_t corresponding to each cluster are assigned a unique positive integer and the remaining elements not belonging to a cluster are assigned zeros. For two configurations Φ_t and $\Phi_{t'}$, we define a measure of similarity J,

$$J(\Phi_t, \Phi_{t'}) = \frac{|\Phi_t \cup \Phi_{t'}|}{51 - \sum_{i=1}^{51} \delta_{0,\Phi_{t,i}\Phi_{t',i}}}, \qquad (9)$$

where $\delta_{x,y}$ is the Kronecker delta function, which is equal to 1 if $x = y$, and 0 otherwise. The ultimate task of globally maximizing $\sum_{t'=1}^{50} \sum_{t=t'+1}^{51} J(\Phi_t, \Phi_{t'})$ is impossible since the number of the parameters in Fig. 4(b) is too large.

To solve the coloring problem, we adopt a heuristic algorithm. We determine the colors of the clusters in reverse from 2011Q4 to 1989Q4. We separate the time period into two intervals: $I_1 = [1989Q4, 1996Q1]$ and $I_2 = [1996Q2, 2011Q4]$. For $t = 2011Q4$ there are three clusters of states colored yellow, green, and red. As we determine Φ_t for a given $t \in I_2$, all $\Phi_{t'}$ with $t' > t$ are already determined. The configuration Φ_t is determined by maximizing $F_2(\Phi_t) = \sum_{\tau=1Q}^{t'} J(\Phi_t, \Phi_{t+\tau})$, where $t' = \min\{6Q, 2011Q4 - t\}$. When $t \in I_1$, we maximize $F_1(\Phi_t) = \sum_{t'=1997Q1}^{1998Q3} J(\Phi_t, \Phi_{t'})$. Note that small alterations in the assigned future reference configuration does not affect the results.

1. Kaminsky, G. L. & Reinhart, C. M. The twin crises: The causes of banking and balance-of-payments problems. *Amer. Econ. Rev.* **89**, 473–500 (2012).
2. Quigley, J. A. Real estate and the Asian crisis. *J. Housing Econ.* **10**, 129–161 (2001).
3. Fung, K.-K. & Forrest, R. Institutional mediation, the Hong Kong residential housing market and the Asian Financial Crisis. *Housing Stud.* **17**, 189–207 (2002).
4. Sanders, A. The subprime crisis and its role in the financial crisis. *J. Housing Econ.* **17**, 254–261 (2008).
5. Giussani, B. & Hadjimatheou, G. Modeling regional house prices in the United Kingdom. *Pap. Reg. Sci.* **70**, 201–219 (1991).
6. Kim, Y. S. & Rous, J. J. House price convergence: Evidence from US state and metropolitan area panels. *J. Housing Econ.* **21**, 169–186 (2012).

7. Pukthuanthong, K. & Roll, R. Global market integration: An alternative measure and its application. *J. Financial Econ.* **94**, 214–232 (2009).
8. Billio, M., Getmansky, M., Lo, A. W. & Pelizzon, L. Econometric measures of systemic risk in the finance and insurance sectors. *J. Financial Econ.* **104**, 535–559 (2012).
9. Kritzman, M., Li, Y.-Z., Page, S. & Rigobon, R. Principal components as a measure of systemic risk. *J. Portf. Manag.* **37**, 112–126 (2011).
10. Tumminello, M., Lillo, F. & Mantegna, R. N. Correlation, hierarchies, and networks in financial markets. *J. Econ. Behav. Org.* **75**, 40–58 (2010).
11. Mantegna, R. N. Hierarchical structure in financial markets. *Eur. Phys. J. B* **11**, 193–197 (1999).
12. Tumminello, M., Aste, T., Di Matteo, T. & Mantegna, R. N. A tool for filtering information in complex systems. *Proc. Natl. Acad. Sci. U.S.A.* **102**, 10421–10426 (2005).
13. Laloux, L., Cizeau, P., Bouchaud, J.-P. & Potters, M. Noise dressing of financial correlation matrices. *Phys. Rev. Lett.* **83**, 1467–1470 (1999).
14. Plerou, V., Gopikrishnan, P., Rosenow, B., Amaral, L. A. N. & Stanley, H. E. Universal and nonuniversal properties of cross correlations in financial time series. *Phys. Rev. Lett.* **83**, 1471–1474 (1999).
15. Drozdz, S., Grümmer, F., Gorski, A. Z., Ruf, F. & Speth, J. Dynamics of competition between collectivity and noise in the stock market. *Physica A* **287**, 440–449 (2000).
16. Song, D.-M., Tumminello, M., Zhou, W.-X. & Mantegna, R. Evolution of worldwide stock markets, correlation structure, and correlation based graphs. *Phys. Rev. E* **84**, 026108 (2011).
17. Sengupta, A. M. & Mitra, P. P. Distributions of singular values for some random matrices. *Phys. Rev. E* **60**, 3389–3392 (1999).
18. Plerou, V. *et al.* Random matrix approach to cross correlations in financial data. *Phys. Rev. E* **65**, 066126 (2002).
19. Pan, R. K. & Sinha, S. Collective behavior of stock price movements in an emerging market. *Phys. Rev. E* **76**, 046116 (2007).
20. Shen, J. & Zheng, B. Cross-correlation in financial dynamics. *EPL (Europhys. Lett.)* **86**, 48005 (2009).
21. Zhou, W.-X. & Sornette, D. Is there a real-estate bubble in the US? *Physica A* **361**, 297–308 (2006).
22. Kenett, D. Y., Shapira, Y. & Ben-Jacob, E. RMT assessments of the market latent information embedded in the stocks' raw, normalized, and partial correlations. *J. Prob. Stat.* **2009**, 249370 (2009).
23. Kenett, D. Y. *et al.* Dominating clasp of the financial sector revealed by partial correlation analysis of the stock market. *PLoS One* **5**, e15032 (2010).
24. Baba, K., Shibata, R. & Sibuya, M. Partial correlation and conditional correlation as measures of conditional independence. *Aust. N. Z. J. Stat.* **46**, 657–664 (2004).
25. Sales-Pardo, M., Guimerà, R., Moreira, A. A. & Amaral, L. A. N. Extracting the hierarchical organization of complex systems. *Proc. Natl. Acad. Sci. U.S.A.* **104**, 15224–15229 (2007).
26. Lancichinetti, A. & Fortunato, S. Consensus clustering in complex networks. *Sci. Rep.* **2**, 336 (2012).
27. Yan, Y., Liu, M.-X., Zhu, X.-W. & Chen, X.-S. Principle fluctuation modes of the global stock market. *Chin. Phys. Lett.* **29**, 028901 (2012).
28. Jiang, X.-F. & Zheng, B. Anti-correlation and subsector structure in financial systems. *EPL (Europhys. Lett.)* **97**, 48006 (2012).
29. Junior, L. S. Cluster formation and evolution in networks of financial market indices. *Algo. Fin.* **2**, 3–43 (2013).
30. Pollakowski, H. & Ray, T. Housing price diffusion patterns at different aggregation levels: An examination of housing market efficiency. *J. Housing Res.* **8**, 107–124 (1997).
31. Noh, J. D. Model for correlations in stock markets. *Phys. Rev. E* **61**, 5981–5982 (2000).
32. Kim, D. H. & Jeong, H. Systematic analysis of group identification in stock markets. *Phys. Rev. E* **72**, 046133 (2005).
33. Newman, M. E. J. & Girvan, M. Finding and evaluating community structure in networks. *Phys. Rev. E* **69**, 026113 (2004).
34. Guimerà, R., Sales-Pardo, M. & Amaral, L. A. N. Modularity from fluctuations in random graphs and complex networks. *Phys. Rev. E* **70**, 025101 (2004).

Acknowledgments

Author contributions

B.P., W.X.Z. and H.E.S. conceived the study. H.M., W.J.X., Z.Q.J., B.P., W.X.Z. and H.E.S. designed and performed the research. H.M., W.J.X. and Z.Q.J. performed the statistical analysis of the data. B.P., W.X.Z. and H.E.S. wrote, reviewed and approved the manuscript.

Additional information